Expansion of scroll wave filaments induced by chiral mismatch

Daniel Weingard, Oliver Steinbock, and Richard Bertram

Citation: Chaos **28**, 045106 (2018); doi: 10.1063/1.5008274
View online: https://doi.org/10.1063/1.5008274
View Table of Contents: http://aip.scitation.org/toc/cha/28/4
Published by the American Institute of Physics

Expansion of scroll wave filaments induced by chiral mismatch

Daniel Weingard,[1] Oliver Steinbock,[2] and Richard Bertram[1,3]
[1]*Department of Mathematics, Florida State University, Tallahassee, Florida 32306-4510, USA*
[2]*Department of Chemistry and Biochemistry, Florida State University, Tallahassee, Florida 32306-4390, USA*
[3]*Programs in Molecular Biophysics and Neuroscience, Florida State University, Tallahassee, Florida 32306-4380, USA*

(Received 4 October 2017; accepted 25 January 2018; published online 3 April 2018)

In three-dimensional excitable systems, scroll waves are rotating vortex states that consist of smoothly stacked spirals. This stacking occurs along one-dimensional phase singularities called filaments. If the system has a positive filament tension, these curves either straighten or collapse over time. The collapse can be prevented if the filament pins to a nonreactive object or a group of objects, but even in this case, the filament length does not typically grow. Using numerical simulations, we provide examples of filament growth induced by pinning, such as a scroll ring pinning to an inert trefoil knot, and explain the mechanism of this growth. Surprisingly, the corresponding filament loop thus not only persists in time but also steadily extends far from the pinning object. *Published by AIP Publishing.* https://doi.org/10.1063/1.5008274

Excitation waves exist in many chemical and biological systems. These waves may form spirals centered at phase singularities in two-dimensional media such as the thin atrial tissue of the human heart, shallow chemical systems, and even bee hives. Three-dimensional analogues of spiral waves are called scroll waves and rotate around a curve called the filament. They appear in the thicker ventricles of the heart and deeper reactive solutions. Previous studies have shown that in systems where scroll waves would collapse, non-reactive objects can stabilize the filament and prevent this collapse. We use computer simulations to show that such objects can, in addition, induce scroll wave expansion. This expansion can result in very complex wave patterns with serious consequences if present in cardiac tissue.

I. INTRODUCTION

Reaction-diffusion systems are capable of sustaining excitation pulses. These pulses are traveling waves with a constant speed and amplitude and are followed by a refractory period that prevents the immediate propagation of a new pulse. Examples in chemistry include concentration waves in autocatalytic reaction-diffusion media,[1] catalytic surface reactions,[2] corrosion processes,[3] and synthetic biochemical networks.[4] Excitation waves organize many mechanisms in biology. These include cell aggregation of social amoebae,[5,6] uterine contractions during labor,[7] voltage waves on heart tissue,[8] defense response waves of honey bee populations,[9] and epidemic outbreaks such as the bubonic plague.[10] At an intracellular level, calcium waves in oocytes prevent polyspermy.[11]

In two spatial dimensions, excitation pulses can break and form vortices in the shape of Archimedean spirals rotating around a central phase singularity, the spiral tip.[12,13] Spiral tips move along specific types of trajectories including circular orbits, epitrochoids, or hypotrochoids.[14] Wave breaks in three dimensions result in scroll waves, which can be thought of as a continuous stack of spiral waves and rotate around one-dimensional phase singularities called filaments. The speed of filament movement not only is approximately inversely proportional to its curvature[15] but is also influenced by higher order effects.[16] The system-specific filament tension, α, causes closed filaments to either shrink ($\alpha > 0$) or expand ($\alpha < 0$). Filaments with negative tension are unstable, which leads to buckling filaments and chaotic wave fields.[17,18] In systems with positive filament tension, filaments may expand due to reactivity gradients[19] or due to spatial confinement.[20] However, neither of these effects lead to chaos.

Static and impermeable heterogeneities impact the behavior of spiral tips and filaments if the respective distance is less than about one wavelength. Filaments have a tendency to wrap around thin heterogeneities, greatly changing the behavior of the wave field. This pinning may prevent filament loops from shrinking in systems with positive filament tension where they would otherwise collapse. More specifically, in experiments with the autocatalytic Belousov-Zhabotinsky (BZ) reaction, filaments were able to wrap around tori or double tori, preventing scroll ring collapse.[21,22] Additional experiments with the BZ reaction revealed that filaments may be sustained by two to four spherical beads, while single spheres do not stop the collapse but extend the life of the loop by up to 25%.[23] Numerical studies inspired by these experiments showed that in a system with randomly placed spherical beads, more and larger beads increased the likelihood of scroll wave persistence.[24]

While previous pinning studies have demonstrated that non-reactive impermeable objects can stop filament collapse, none have reported filament expansion. We present a novel mechanism for scroll ring expansion in a system of positive filament tension where pinning to heterogeneities induces the expansion. Using a simple, two-variable excitable system model and parallel computing with a programmable graphics processing unit (GPU), we show that scroll ring expansion

can be induced by pinning to a knotted object. The topology of the knot induces chiral mismatch in the wave rotation about the pinned filament. We demonstrate that a similar mismatch can occur on a topologically simpler torus by initiating two scroll rings of opposite chirality. In both cases, the chiral mismatch is responsible for persistent filament expansion and the consequent complex wave pattern.

II. METHODS

Our simulations employ the Barkley model[25] which is commonly used to describe excitable reaction-diffusion systems. The model is given by the following dimensionless equations:

$$\frac{\partial u}{\partial t} = D_u \Delta u + \epsilon^{-1} u(1-u)\left(u - \frac{v+b}{a}\right), \tag{1}$$

$$\frac{\partial v}{\partial t} = D_v \Delta v + u - v, \tag{2}$$

where u and v are bound by $0 \le u, v \le 1$. In the context of the BZ reaction, the variables u and v are similar to the concentrations of bromous acid and the oxidized form of ferroin.[22] The system parameters ϵ, a, and b are 0.02, 1.1, and 0.18, respectively. The diffusion coefficients are $D_u = D_v = 1$. This choice of parameters allows for scroll waves with positive filament tension which have no movement in the binormal direction.[26] We integrate using the forward Euler method with a seven point finite difference scheme to discretize the Laplacian. Non-reactive impermeable cylindrical surfaces are inserted into the domain before the initial conditions are set. These objects are discretized by voxels of size $0.2 \times 0.2 \times 0.2$. The minor radius of each surface is 1.0. The major radius of each torus is 22.8. The inner curve of the trefoil knot is given by the following equation (and illustrated in Fig. 1):

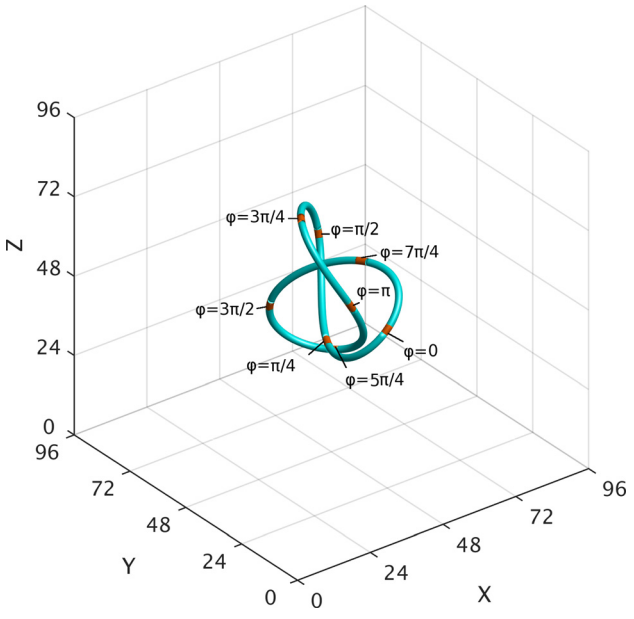

FIG. 1. A trefoil knot and its parametrization by φ.

$$\begin{cases} 0 \le \varphi \le 2\pi \\ X = 48 - 5\sin 3(\pi - \varphi), \\ Y = 48 - [2\cos 2(\pi - \varphi) - \cos(\pi - \varphi)], \\ Z = 48 - [2\sin 2(\pi - \varphi) - \sin(\pi - \varphi)]. \end{cases} \tag{3}$$

The system boundary and the boundary with the inert objects obey no-flux (Neumann) boundary conditions. Simulations are performed on a $480 \times 480 \times 480$ grid with a spacing and time step of 0.2 and 0.005, respectively.

We parallelize our solver by sectioning the domain into a $60 \times 60 \times 60$ grid of blocks. Single blocks are processed by a warp of the GPU and contain an $8 \times 8 \times 8$ grid of points. Each point is processed by a thread within a warp, where a thread can share information within its warp and each point on a block's boundary shares information with the warp for the adjacent block.

Each simulation is initiated with an expanding spherical wave with the following equations:

$$\begin{cases} u = 0.95 & 1 \le r \le 4, \\ u = 0 & \text{otherwise}, \end{cases} \tag{4}$$

$$\begin{cases} v = \dfrac{0.6}{6 - 5r} & 0 \le r < 1, \\ v = \dfrac{0.9(20 - 5r)}{15} & 1 \le r \le 4, \\ v = 0 & \text{otherwise}, \end{cases} \tag{5}$$

where r is the distance from the center of the expanding spherical wave. At $t = 4$ and if y is smaller than the value of y in the center of the expanding spherical wave, we set $u = 0$ and $v = 0$; otherwise, the values of u and v remain unchanged. This creates a single scroll ring with a circular filament that in the absence of further perturbation does not move in the binormal direction but shrinks and eventually collapses due to positive filament tension. We define a point to be on the filament if $u = 0.5$ and $v = \frac{a}{2} - b$ and track it with the marching cube algorithm.[22,27]

III. RESULTS

We first simulate a scroll ring collapsing onto a trefoil knot. Figure 2 depicts the wave field (orange) as it starts to interact with the knot (cyan). The scroll ring is only partially shown to facilitate visualization. Subsequently, the wave structure transforms from a bowl shape [Fig. 2(a)] to an extremely complex pattern with wave rotations occurring far from the knot [Fig. 2(b)]. This expansion is entirely unexpected because filaments in this system should shrink due to positive filament tension, and so, the expansion must be induced by interaction with the inert knot.

Figure 3 illustrates how the filament interacts with the trefoil knot over time. The simulation is initialized with the filament surrounding the knot [Fig. 3(a)]. As the filament collapses, two antipodal regions contact the knot and the waves locally rotate around it, while the remainder begins to deform [Fig. 3(b)]. We represent the contact regions as green or blue sections on the object, where each color represents a

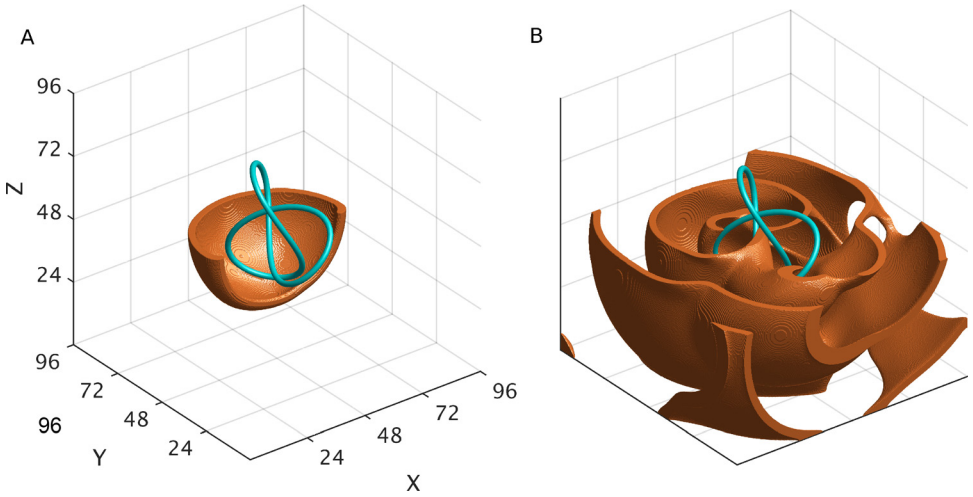

FIG. 2. A scroll ring pinning to an inert trefoil knot. Orange represents $u > 0.3$. The trefoil knot is shown in cyan. (a) The scroll ring is near its initial condition before its first rotation. Only the lower back portion of the wave is shown. (b) The scroll ring has developed a very complicated wave pattern after 247 rotations. Only the lower portions of the waves are shown.

different rotational chirality. That is, the direction of rotation around the green portion of the knot is opposite to that around the blue portion. Later, two additional contact regions appear and all four regions begin to wrap around the knot [Fig. 3(c)]. Eventually, the filament surrounds the majority of the knot and the free parts collide with the boundary. Each of the four contact regions emits two arms of the filament that connect the trefoil to the boundary [Fig. 3(d)]. Later, two pairs of arms coalesce and pinch off the trefoil, leaving four arms of the filament at the ends of two contact regions [Fig. 3(e)]. The filament appears to remain in this arrangement indefinitely (the simulation ends after 1800 rotations). This demonstrates that scroll wave pinning to a knotted object can induce filament expansion, even in a system with positive filament tension.

To understand this expansion, we explore a simpler case where a scroll ring pins to a torus. We initialize the scroll ring so that the circular filament (with radius one third the size of the torus' major radius) exists in the same plane as the torus that it intersects [Fig. 4(a)]. The part of the filament inside the torus collapses and pins to the torus (green), while the outer portion remains a free loop [Fig. 4(b)]. Just like with the trefoil knot, the contact region starts to self-wrap around the torus and the free part expands [Fig. 4(c)]. Eventually, the filament completely wraps around the torus and the free part pinches off [Fig. 4(d)]. Afterwards, the free part exists as a loop and drifts away [Fig. 4(e)], eventually vanishing at the boundary. At this point in time, the scroll wave is organized about the filament which is completely pinned to the torus [Fig. 4(f)].

Why does the filament initially expand? Why does the free part move away from the torus after pinching off? To answer these questions, we examine the spiral waves in a two-dimensional slice of the three-dimensional system where a scroll ring pins to a torus (Fig. 5). In this slice, the torus appears as two circles (blue), the wave front (white) initially has a U shape with one end point near the inside of the torus and the other end point outside of the torus. Both these end points are spiral tips (red) [Fig. 5(a)]. The part of the wave inside of the torus collapses onto it (right blue point) and rotates with a frequency of $\nu = 0.12$. The spiral tip outside of

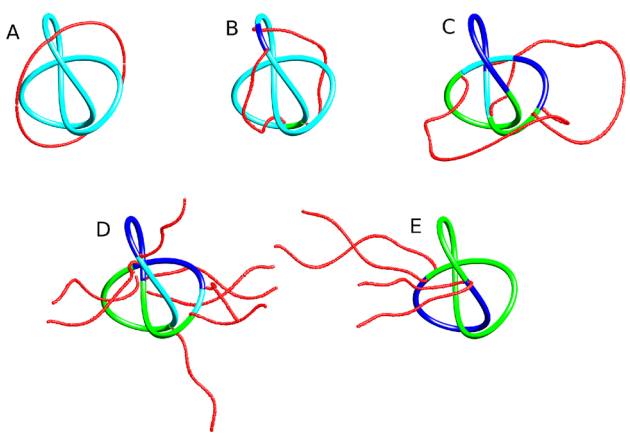

FIG. 3. A scroll ring pinning to an inert trefoil knot (cyan). Only the filament is shown. Red represents the free filament. Blue and green represents the pinned filament with differing chirality. (a) The filament of the scroll ring before its first rotation. (b)–(e) The filament after approximately 12, 38, 247, and 448 rotations.

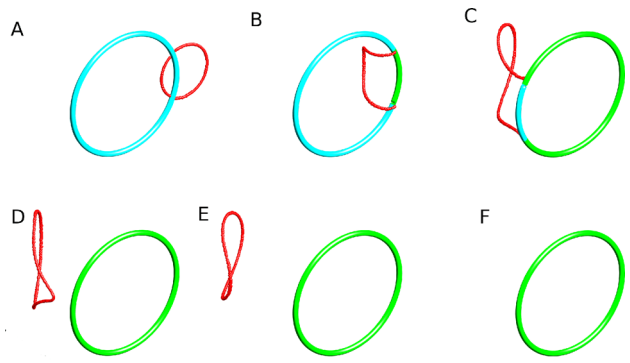

FIG. 4. A scroll ring pinning to a torus (cyan). Only the filament is shown. Red represents the free filament. Green represents the pinned filament. (a) The scroll ring filament before the first rotation. (b)–(f) After approximately 23, 42, 47, 53, and 79 rotations.

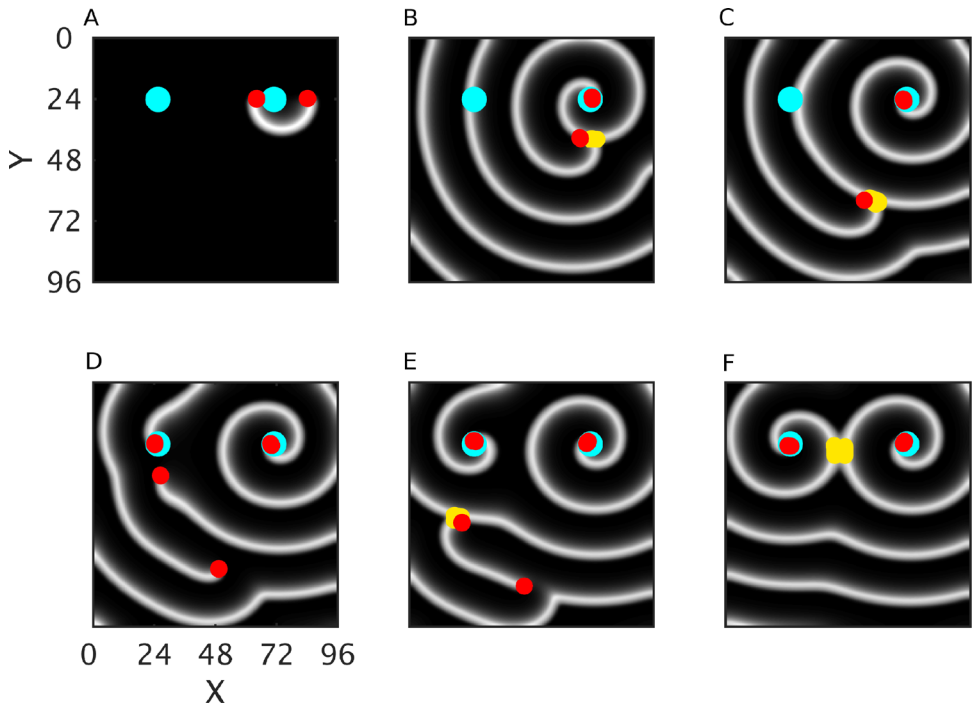

FIG. 5. Scroll ring pinning to a torus illustrated by two-dimensional slices at $z = z_{center}$ (the z value in the center of the initial, expanding sphere) of a scroll ring pinning to a torus. v is shown where white represents the high v values. Blue circles represent the slices of the torus. Red represents the spiral tip. Yellow represents the wave collisions. (a) The scroll ring before its first rotation. (b)–(f) After approximately 23, 42, 47, 53, and 79 rotations.

the torus rotates with a lower frequency of $\nu = 0.09$. Both these phase singularities emit waves that annihilate each other upon collision (yellow). Since the pinned spiral tip rotates faster than the unpinned tip, the frequent waves that are emitted cause wave collisions that push the free spiral back [Figs. 5(a)–5(c)]. When the filament completely wraps around the torus, there is a second pinned spiral tip in the two-dimensional slice that coincides with the left blue point [Fig. 5(d)]. The free filament is now a closed curve, reflected as two red points in the two dimensional slice. Both free spiral tips are pushed out of the boundary from wave collisions [Figs. 5(e) and 5(f)]. This phenomenon of wave collisions causing spiral tip drift has been documented in two-dimensional systems.[28] We also note that pinning to thick obstacles decreases the rotation frequency as reported earlier,[21] but a study using the Barkley model has shown that thin heterogeneities can increase the frequency as in our case.[29]

We also investigated the vortex dynamics in the presence of a thick toroidal heterogeneity because in this case the rotation frequency about the object should be lower. If we increase the minor radius of the torus by a factor of three ($r = 3.0$), a pinned scroll wave rotates around it with a frequency of $\nu = 0.08$. Because this is slightly less than the frequency of the free scroll wave, we predicted that the waves that propagate from a pinned section of the filament should not be able to push back the free filament. Just as before, we initialize a circular filament that intersects a torus, this time with a minor radius of $r = 3.0$ [Fig. 6(a)]. It rapidly collapses [Fig. 6(b)], and ultimately, all waves disappear and the entire system approaches its spatially homogeneous steady state [Fig. 6(c)]. We also studied the situation of a thick trefoil knot with $r = 3.0$ [Fig. 6(d)]. The filament attaches to the knot [Fig. 6(e)] but eventually completely collapses, leaving the system in its steady state free of wave activity [Fig. 6(f)]. These simulations match our expectations and show that a sufficiently thin heterogeneity is necessary to induce filament expansion.

While filament expansion is transient in the case of the tori (Fig. 4), it persists when the filament is attached to a trefoil knot (Fig. 3). This occurs because the expanding filament ultimately detaches from the torus, but not the trefoil. What is the reason for this difference? Filaments attached to a nonreactive cylindrical object rotate with a particular

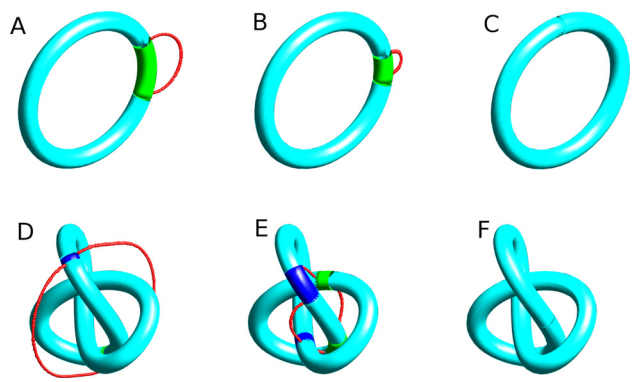

FIG. 6. Thick cylindrical surfaces ($r = 3.0$) do not induce filament expansion. Only the filament is shown. Red represents the free filament. Blue and green represent the pinned filament with differing chirality. (a) A scroll ring collapsing onto a thick torus before its first rotation. (b) After two rotations, the length of the pinned and free filament has declined. (c) After three rotations, the system is near a spatially homogeneous steady state. (d) A scroll ring collapsing onto a thick trefoil knot before its first rotation. (e) After 13 rotations, the filament has begun to pin to the knot, but the filament length has decreased. (f) After 20 rotations, the system is near a spatially homogenous steady state.

chirality around it. When the ends of the filament meet on the torus, both rotate with the same chirality and can coalesce. However, in the case of a trefoil knot, this meeting involves different rotational chirality.

Figure 7(a) shows a chirality plot that, for each rotation number, shows the chirality of the attached portion of the filament (green or blue) with the unattached portion (cyan) separating green and blue regions. This analysis is performed in terms of the parameter φ that describes the position on the trefoil knot. Subsequent panels show the full trefoil and filament at time points corresponding to the vertical red lines in panel A. After 12 rotations (panel B), there are only two small attached regions of opposite chirality. These both grow in time, and two new chiral regions appear soon after. Such an arrangement persists for many rotations, with the 8-armed free filament shown in panel C. This structure contains a cyan region surrounding $\varphi = \pi$. Eventually, the free filament comes into contact with this cyan region (panel D), which results in a new blue region (panel E). At the same time, the blue region at $\frac{3\pi}{2} < \varphi < 2\pi$ shrinks as the surrounding green region expands (panel D). This blue region detaches from the trefoil allowing the surrounding green regions to coalesce, releasing two pairs of filament arms (panel E). Over time, the blue region at $\pi < \varphi < \frac{3\pi}{2}$ expands, while the blue region at $\frac{\pi}{2} < \varphi < \pi$ contracts (panel F). Ultimately, the blue region at $\frac{\pi}{2} < \varphi < \pi$ collapses, releasing a pair of filament arms. Two contact regions of opposing chirality with two pairs of filament arms remain on the trefoil knot and appear to persist indefinitely (panel G). We hypothesize that this difference in rotational orientation stops the final two contact regions from combining and thus prevents the free parts of the filament from detaching off of the trefoil knot.

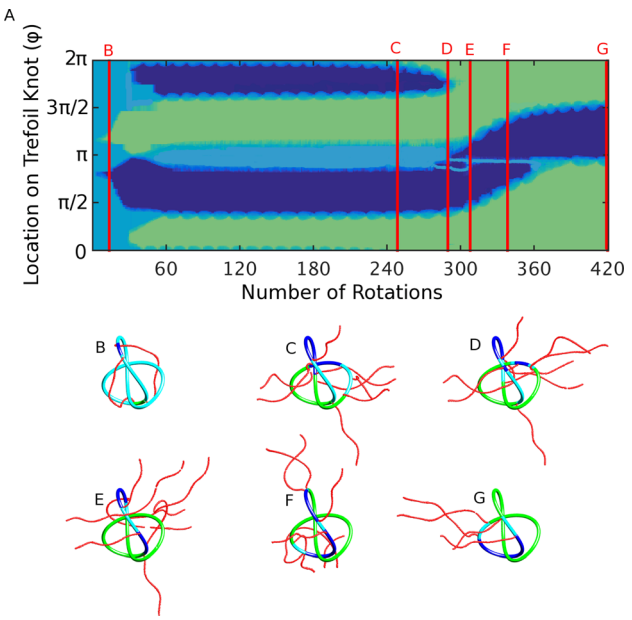

FIG. 7. (a) Chirality plot in terms of the location parameter φ. Cyan represents the knot segments that are filament-free, and blue and green indicate the segments with the filament of opposing chirality. The cyan, blue, and green in (a) correspond to cyan, blue, and green in (b)–(g). The red lines depict when (b)–(g) occur. (b)–(g) The filament interacting with the trefoil knot after 12, 247, 286, 305, 340, and 420 rotations, respectively.

We test this hypothesis by simulating two separate scroll rings with opposite chirality diametrically opposed on a torus [Fig. 8(a)]. Each filament has a pinned part that wraps around the torus and a free part that expands [Fig. 8(b)]. The expansion continues until each chiral region covers half of the torus. Because of their opposing chirality, they fail to coalesce, and the pinned regions cause the free parts to expand [Fig. 8(c)]. Eventually, the free parts hit the boundary, leaving four free arms connecting the torus to the boundary [Fig. 8(d)]. These arms appear to remain indefinitely. This numerical experiment reveals that opposing chirality of self-wrapping filaments is sufficient to create an expanding filament that remains attached to the pinned object. In this way, the filament can continue to expand indefinitely.

To further test the hypothesis that expanding filaments are the product of chiral mismatch, we simulate two scroll rings with the same chirality initiated at opposite ends of a torus [Fig. 9(a)]. Each filament has a pinned part (green) that wraps around the torus and an expanding free part (red) [Fig. 9(b)]. When both filaments with the same chirality meet, they combine and the free part detaches from the torus [Fig. 9(c)]. The free scroll ring shrinks as it drifts away from the torus [Fig. 9(d)]. Finally, the free scroll ring annihilates at the boundary of the system, leaving behind a scroll ring completely pinned to the torus [Fig. 9(e)]. Without opposing chirality, the free parts of the scroll ring filaments were unable to expand indefinitely.

IV. CONCLUSIONS

We have shown that an inert trefoil knot, when placed in the center of a scroll ring, may induce filament expansion. This phenomenon occurs because as the filament collapses, part of it pins to the knot and the rest remains free. The pinned part of the filament rotates faster than the free part and thus emits waves at a higher rate. The waves originating from the pinned filament annihilate the waves originating from the free filament. Eventually, waves from the pinned filament reach the free filament and push it back. We confirmed that these collisions are actually capable of moving filaments in three dimensions by simulating a scroll ring partially pinned to a torus. Two-dimensional slices of the simulation revealed that this three-dimensional collision-induced expansion is analogous to a well-documented two-dimensional phenomenon where spiral tips can be pushed by spiral wave fronts originating from faster rotating spirals.[28,30]

When the filament partially pins to a torus, it wraps around it and the unpinned part eventually separates from

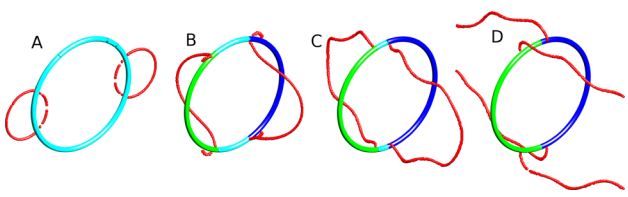

FIG. 8. Two scroll ring filaments with opposite chirality pin to a torus from opposite ends. Red represents the free filament. Blue and green represents the pinned filament with differing chirality. (a) The scroll rings before their first rotation. (b)–(d) Following approximately 29, 42, and 58 rotations. Free filament arms persist.

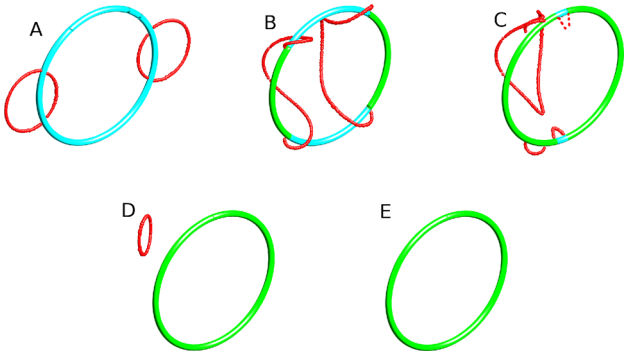

FIG. 9. Two scroll ring filaments with matching chirality pinned to a torus from opposite ends. Red represents the free filament. Green represents the pinned filament. (a) The scroll ring before its first rotation. (b)–(e) Following approximately 29, 33, 37, and 56 rotations. There is no free filament after 56 rotations.

the torus. At this point, the free part is completely disconnected from the torus, stops expanding, and collapses while being pushed towards the boundary. When pinning to a trefoil knot, the filament attaches to the knot at multiple locations and rotates around it with opposing chirality. The filament self-wraps around the knot, and the different pieces of the filament eventually meet. Adjacent filaments with different chirality cannot combine and remain as free filaments. This allows the free part of the filament to continue to expand until it hits the system boundary. We highlight the importance of opposing chirality with two simulations of two scroll rings partially pinned to a single torus. When they had mismatched chirality, the filament expanded until it reached the system boundary. If these simulations existed in an unbound system, we predict that the filament would continue to expand indefinitely. When chirality matched, both filaments combined, allowing the free part of the filament to disconnect from the torus and collapse.

In addition to these results, we explored how the filament interacts with a trefoil knot when the initial condition has only one contact point (not shown). This leads to additional contacts and persistent free filament arms. We also explored how a scroll wave organizes about a figure eight knot. As with the trefoil, this resulted in multiple chirality regions and persistent free filament arms (not shown).

Our results provide concrete predictions for experiments with the BZ reaction, specifically that partial pinning to thin cylindrical surfaces can lead to scroll ring expansion. The experimental verification of these predictions in chemical experiments seems to be feasible because small inert tori have been successfully used in previous studies to induce scroll wave pinning and BZ systems typically show positive filament tension. These earlier studies also developed methods for the initiation of scroll rings with controlled initial radii at predetermined locations.[21,31] In addition, inert trefoil knots and similar heterogeneities could be constructed using a 3-D printer. Challenges, however, include the limited lifetime of wave patterns in closed BZ systems and the analysis of the complicated wave fields around the knot.

Finally, our study could provide insights into certain cardiac arrhythmias. Ventricular tachycardia (VT), an increased rhythm in the heart originating in the ventricles, can be caused by a large rotating wave in the thick, three-dimensional tissue. If the behavior of this wave becomes chaotic ventricular tachycardia transitions to fibrillation (VF).[32] Negative filament tension is a well-documented mechanism of filament growth that leads to chaotic wave fields and is a likely cause for the transition of VT to VF.[33] Simulations with cardiac models could test whether the dynamics discussed in this paper are relevant to ventricular tachycardia and fibrillation.

ACKNOWLEDGMENTS

This work was supported by the National Science Foundation under Grant No. CHE-1565734 to O.S. and Grant No. DMS-1220063 to R.B. Special thanks to Wilfredo Blanco for discussion and technical assistance. We are grateful to Jack Hudson for his pioneering research on spatiotemporal pattern formation in chemical systems.

[1]I. R. Epstein and J. A. Pojman, *An Introduction to Nonlinear Chemical Dynamics: Oscillations, Waves, Patterns, and Chaos* (Oxford University Press, New York, 1998).
[2]G. Ertl, "Reactions at surfaces: From atoms to complexity (Nobel lecture)," Angew. Chem., Int. Ed. Engl. **47**, 3524–3535 (2008).
[3]K. Agladze and O. Steinbock, "Waves and vortices of rust on the surface of corroding steel," J. Phys. Chem. A **104**, 9816–9819 (2000).
[4]A. S. Zadorin, Y. Rondelez, J.-C. Galas, and A. Estevez-Torres, "Synthesis of programmable reaction-diffusion fronts using DNA catalyzers," Phys. Rev. Lett. **114**, 068301 (2015).
[5]K. J. Lee, E. C. Cox, and R. E. Goldstein, "Competing patterns of signaling activity in Dictyostelium discoideum," Phys. Rev. Lett. **76**, 1174 (1996).
[6]A. J. Durston, "Dislocation is a developmental mechanism in Dictyostelium and vertebrates," Proc. Natl. Acad. Sci. U.S.A. **110**, 19826–19831 (2013).
[7]E. Pervolaraki and A. V. Holden, "Spatiotemporal patterning of uterine excitation patterns in human labour," Biosystems **112**, 63–72 (2013).
[8]J. M. Davidenko, A. V. Pertsov, R. Salomonsz, W. Baxter, and J. Jalife, "Stationary and drifting spiral waves of excitation in isolated cardiac muscle," Nature **355**, 349–351 (1992).
[9]G. Kastberger, E. Schmelzer, and I. Kranner, "Social waves in giant honeybees repel hornets," PLoS One **3**, e3141 (2008).
[10]J. D. Murray, *Mathematical Biology. II Spatial Models and Biomedical Applications*, Interdisciplinary Applied Mathematics Vol. 18 (Springer-Verlag, 2001).
[11]M. J. Berridge, "Inositol trisphosphate and calcium signalling mechanisms," Biochem. Biophys. Acta **1793**, 933–940 (2009).
[12]A. T. Winfree, "Spiral waves of chemical activity," Science **175**, 634–636 (1972).
[13]O. Steinbock and S. C. Müller, "Chemical spiral rotation is controlled by light-induced artificial cores," Physica A **188**, 61–67 (1992).
[14]A. T. Winfree, "Varieties of spiral wave behavior: An experimentalist's approach to the theory of excitable media," Chaos **1**, 303–334 (1991).
[15]J. P. Keener, "The dynamics of three-dimensional scroll waves in excitable media," Physica D **31**, 269–276 (1988).
[16]B. Marts, T. Bánsági, Jr., and O. Steinbock, "Evidence for Burgers' equation describing the untwisting of scroll rings," Europhys. Lett. **83**, 30010 (2008).
[17]V. Biktashev, A. Holden, and H. Zhang, "Tension of organizing filaments of scroll waves," Philos. Trans. R. Soc. A **347**, 611–630 (1994).
[18]S. Alonso, F. Sagués, and A. S. Mikhailov, "Taming Winfree turbulence of scroll waves in excitable media," Science **299**, 1722–1725 (2003).
[19]T. Amemiya, P. Kettunen, S. Kádár, T. Yamaguchi, and K. Showalter, "Formation and evolution of scroll waves in photosensitive excitable media," Chaos **8**, 872–878 (1998).
[20]J. F. Totz, H. Engel, and O. Steinbock, "Spatial confinement causes lifetime enhancement and expansion of vortex rings with positive filament tension," New J. Phys. **17**, 093043 (2015).
[21]Z. A. Jimènez, B. Marts, and O. Steinbock, "Pinned scroll rings in an excitable system," Phys. Rev. Lett. **102**, 244101 (2009).

[22]S. Dutta and O. Steinbock, "Topologically mismatched pinning of scroll waves," J. Phys. Chem. Lett. **2**, 945–949 (2011).
[23]Z. Jiménez and O. Steinbock, "Pinning of vortex rings and vortex networks in excitable systems," Europhys. Lett. **91**, 50002 (2010).
[24]D. Weingard, W. Blanco, O. Steinbock, and R. Bertram, "Stabilization of collapsing scroll waves in systems with random heterogeneities," Chaos **27**, 043108 (2017).
[25]D. Barkley, "A model for fast computer simulation of waves in excitable media," Physica D **49**, 61–70 (1991).
[26]S. Alonso, R. Kähler, A. S. Mikhailov, and F. Sagués, "Expanding scroll rings and negative tension turbulence in a model of excitable media," Phys. Rev. E **70**, 056201 (2004).
[27]W. E. Lorensen and H. E. Cline, "Marching cubes: A high resolution 3D surface construction algorithm," in *SIGGRAPH '87 Proceedings of the Annual Conference on Computer Graphics and Interactive techniques* (ACM, New York, 1987), Vol. 21, pp. 163–169.
[28]F. Xie, Z. Qu, J. N. Weiss, and A. Garfinkel, "Interactions between stable spiral waves with different frequencies in cardiac tissue," Phys. Rev. E **59**, 2203 (1999).
[29]F. Spreckelsen, D. Hornung, O. Steinbock, U. Parlitz, and S. Luther, "Stabilization of three-dimensional scroll waves and suppression of spatio-temporal chaos by heterogeneities," Phys. Rev. E **92**, 042920 (2015).
[30]V. Krinsky and K. Agladze, "Interaction of rotating waves in an active chemical medium," Physica D **8**, 50–56 (1983).
[31]Z. A. Jiménez and O. Steinbock, "Stationary vortex loops induced by filament interaction and local pinning in a chemical reaction-diffusion system," Phys. Rev. Lett. **109**, 098301 (2012).
[32]J. N. Weiss, P.-S. Chen, Z. Qu, H. S. Karagueuzian, and A. Garfinkel, "Ventricular fibrillation: How do we stop the waves from breaking?," Circ. Res. **87**, 1103–1107 (2000).
[33]A. Karma, "Physics of cardiac arrhythmogenesis," Annu. Rev. Condens. Matter Phys. **4**, 313–337 (2013).